

# Translocation of polymer chains through interacting nanopores

Meng-Bo Luo

*Department of Physics, Zhejiang University, Hangzhou, Zhejiang 310027, China*

Received 11 July 2007; received in revised form 15 September 2007; accepted 28 October 2007

Available online 1 November 2007

## Abstract

The effect of the interaction between nanopore and chain segment on the translocation of polymer chains through an interacting nanopore from a confined environment (*cis* side, high concentration of chain) to a spacious environment (*trans* side, zero concentration) was studied by using dynamic Monte Carlo simulations. Results showed that a moderate attractive pore–polymer interaction accelerates the translocation of chain. The optimal interaction at which translocation is the fastest increases with the concentration of chain on the *cis* side. The dependence of microscopic behaviors of chain translocation on the interaction was investigated.

© 2007 Elsevier Ltd. All rights reserved.

*Keywords:* Translocation; Nanopore; Interaction

## 1. Introduction

The mechanism of polymers or macromolecules translocating through nanotubes or nanopores in membranes has attracted a lot of attention from experiments [1–4], analytical theories [5–12] and computer simulations [13–23]. The translocation of chain molecule is a fundamental event in various biological processes, such as proteins transporting through channels in biological membranes [24–26], RNA molecules translocating through pores in cell nuclear membranes, DNA molecules transferring from virus to host cell and genes transferring between bacteria [27]. It also relates to the migration of DNAs through microfabricated channels and devices [28–32], gene therapy, drug delivery, gel electrophoresis [33,34], and size exclusion chromatography [35]. When the size of chain molecule is larger than that of the cross section of nanopore, the chain suffers a free energy barrier because it must lose entropy in order to cross the nanopore. Polymer chains also suffer similar free energy barrier in a restrictive environment such as in a gel, in periodic gaps [36] or in random media [37]. Because of the free energy barrier, most translocation phenomena of chain require the aid of driving forces. A topic

related to the translocation of chain through nanopore under driving forces is interesting and important.

Nanopore without considering its thickness is easier to be treated in theory and thus has attracted a lot of attention. The translocation of polymer chain through a non-interacting nanopore has been well studied by theory based on one-dimensional driven-diffusion system [5,8]. The mechanism of chain translocation was discussed based on the free energy barrier  $F_b$  caused by nanopore and chemical potential difference  $\Delta\mu$  between *cis* and *trans* sides [5,8]. In these discussions  $\Delta\mu$  serves as a driving force. Later, the translocation of polymer chain driven by an electric field for a three-dimensional system was simulated, and results showed that the behavior could be described by one-dimensional Smoluchowski equation with chain length independent diffusion constant [13]. The chemical potential difference  $\Delta\mu$  can be set up by concentration difference, and it increases gradually with the increase of the concentration difference [38]. The effect of concentration difference on the translocation was also studied for chain confined in a sphere [14]. Besides the chemical potential difference and electric field, the translocation can also be driven by ratchet mechanism [6,39]. An attractive interaction on the *trans* side of the membrane was recently demonstrated to be a driving force for translocation. It was found that chain worms through nanopore easily for the attractive interaction

*E-mail address:* [luomengbo@zju.edu.cn](mailto:luomengbo@zju.edu.cn)

larger than an adsorption threshold, a critical point at which chain goes from a ‘mushroom’ expanded state to a ‘pancake’ adsorbed state [15,16]. The influence of surface curvature near the nanopore on the translocation of chain was also simulated with off-lattice Monte Carlo technique [18].

However, the effect of interaction between nanopore and polymer on the translocation is not clear. A Brownian dynamic simulation study showed that the interaction affects the translocation time of chain but the details were not stated [11]. In a recent simulation study on a charged polymer translocation through a nanopore with finite length under the application of an electric field, the interaction between polymer and pore was taken into account [17]. The influence of charge and field strength on the polymer translocation was discussed but the influence of pore–polymer interaction was not mentioned. Some experiments also implied that the interaction might play an important role on the translocation of chain through small pore or narrow channel [1,2,40]. The present work studies the effect of the pore–polymer interaction on the translocation of chains from a high concentration region (*cis* side) to zero concentration region (*trans* side). Therefore the model system is not symmetrical for chains on the *cis* and *trans* sides. The dependence of the translocation time on the interaction is investigated. We find that the translocation time exhibits a minimum as the attractive interaction is increased. That is, a proper pore–polymer interaction can drive chains through nanopores.

## 2. Model and simulation method

Our simulation system is embedded in the simple cubic (SC) lattice. The simulated box is a cuboid with spacing  $L_x$ ,  $L_y$  and  $L_z$  in  $x$ ,  $y$  and  $z$  directions, respectively. Periodic boundary conditions (PBC) are considered in the  $x$  and  $y$  directions, while in the  $z$  direction there are two infinitely large flat walls located at  $z = 0$  and  $L_z + 1$ , respectively. The space between these two impenetrable walls is called *cis* side and polymers are confined on the *cis* side before translocation. A nanopore

is located at the center of the upper wall at  $z = L_z + 1$  through which polymer chains can escape from the *cis* side. Above the upper wall, there is an infinite large space and no chain in simulation. This half infinite space is called *trans* side. A sketch of our model system is given in Fig. 1. The size of pore is only one lattice site in the present simulations.

A polymer chain of length  $n$  is comprised of  $n$  self-avoiding identical segments and each segment occupied one lattice site. Bond length between two sequential segments equals the lattice constant, which is set as the unit of length. The interaction between segments and that between segment and surface are supposed to be self-avoiding. We introduced a pore–polymer interaction between the circum of pore and polymer segment since the pore can be constructed by other materials in natural or artificial membranes. An interaction  $E$  is assigned for every nearest neighbor pair of polymer segment and circum of pore, as shown in Fig. 1. The reduced interaction  $\varepsilon = E/k_B T$  is used in the work with  $k_B$  the Boltzmann constant and  $T$  the temperature.

The dynamics of polymer chains includes local and global Brownian movements. The method was discussed in detail by Gurler et al. [41] earlier and the simulation details can be found in our recent papers [19,38,42]. The local movement contains three elementary motions of segments: the end rotation,  $90^\circ$  crankshaft rotation and kink jump motion. While for global movement, slithering snake-like reptation is considered for two end segments: every attempted reptation leads the whole chain to move one lattice forward or backward. For every end segment, the probability for choosing reptation is arbitrarily set to be 0.5. The trial move will be accepted with a probability  $p = \min(1, e^{-\Delta E/k_B T})$  if the self-avoidance is satisfied. Here  $\Delta E$  is the energy change for each trial move. By the local and global movements polymer chains change their configurations as well as spatial locations.

At the beginning of every simulation run, we close the nanopore and put  $N$  identical chains of length  $n$  on the *cis* side. The corresponding concentration  $C$  of chain is defined as volume fraction of segment on the *cis* side before translocation, i.e.,

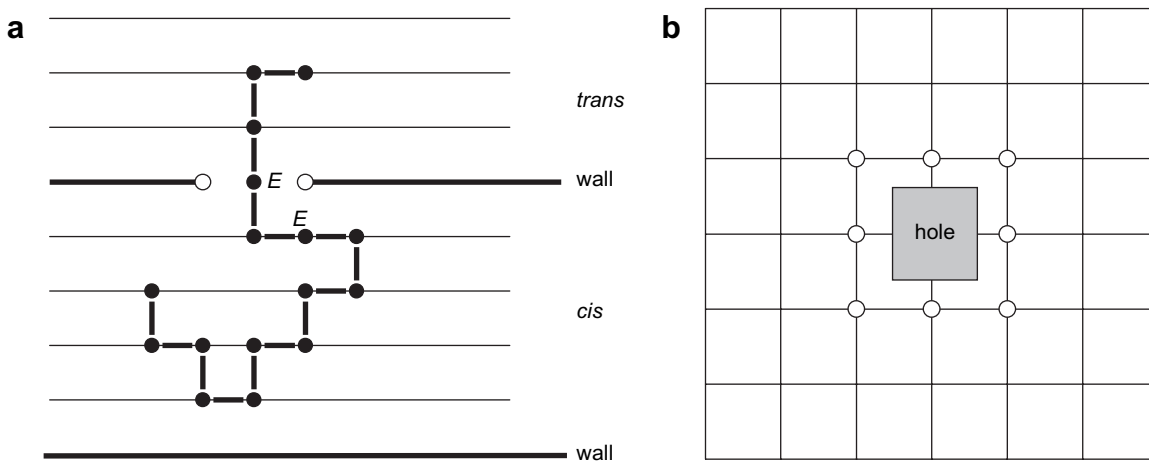


Fig. 1. Sketch of our simulation model: (a) side view: the upper wall with a nanopore at center separates the *cis* side and the *trans* side. Polymer, represented by connected beads, can translocate through the pore. An interaction energy  $E$  is assigned to each nearest neighbor pair of polymer segment and circum of pore; (b) top view: the structures of pore and the circumference of pore. The pore is marked by gray and the circum is marked with open circles.

$C = Nn/V$  with  $V = L_x \times L_y \times L_z$  the total lattice sites in the *cis* side. The time unit is one Monte Carlo step (MCS) during which  $Nn$  trail movements are attempted. We assume the system reaches equilibrium state after  $10n^2$  MCS Brownian movements since it is much longer than the correlation time  $0.25n^{2.13}$  MCS for single SAW chain in free space [33]. Then we open the pore on the upper wall and monitor the translocation of chains through the pore. The moment of opening the pore is set as the starting time  $t = 0$ .

A certain time later, one of the chains reaches the pore and several front segments of the chain worm out of the *cis* side by randomly forth and back motion. But this step does not necessarily lead to a successful escape; segments on the *trans* side may be pulled back totally by an entropic force because the chain is in an entropically unfavoured state when it enters the nanopore [8]. After the trial escape the chain may go back into the *cis* side again. Nevertheless, a final successful escape occurs after several trial escapes.

We have monitored the motion of each chain on the *cis* side. The moment we open the pore is set as  $t = 0$ . The elapsed time from opening the pore to a first successful escape is called the translocation time  $\tau$ . The whole translocation process can be divided into two time scales: the elapsed time for the final successful escape is named escaping time  $\tau_2$ , while that before the final successful escape is named relaxation time  $\tau_1$ . Therefore we have

$$\tau = \tau_1 + \tau_2. \quad (1)$$

Specifically, during the escaping time  $\tau_2$  the chain successfully worms through the pore without totally pulled back. The name ‘escaping time’ for  $\tau_2$  is followed the definition of Muthukumar [14]. However, there are several different names for  $\tau_2$  in literature, such as ‘residence time’ [8], ‘sliding time’ [18], and ‘translocation time’ [5].

To calculate the relaxation time  $\tau_1$  and the escaping time  $\tau_2$ , we monitor the number of segments out of the box,  $n_{\text{out}}$ , at every MC step. Fig. 2 presents the change of  $n_{\text{out}}$  at different

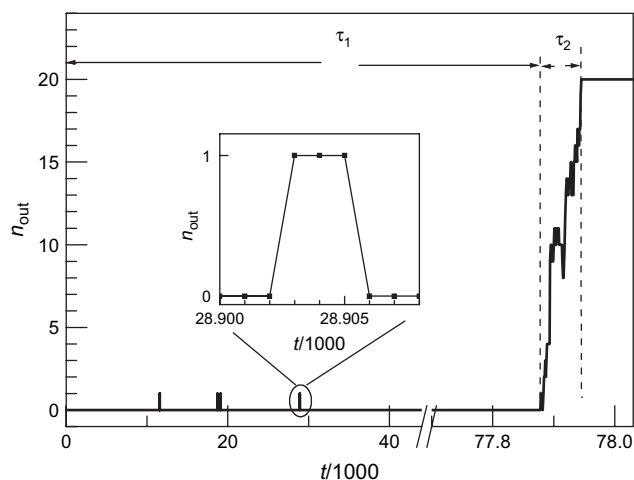


Fig. 2. The variation of the number of segments out of the box,  $n_{\text{out}}$ , with time  $t$  for a multi-chain system  $N = 50$  with interaction  $\varepsilon = 0$ . Here  $\tau_1$  is the relaxation time and  $\tau_2$  is the escaping time. The inset presents one trial escape.

MC steps for a multi-chain system ( $N = 50$ ) with interaction  $\varepsilon = 0$ . Here,  $n_{\text{out}} = 0$  means that the chain is on the *cis* side while  $n_{\text{out}} = n$  represents a successful escaping event. A process with nonzero values of  $n_{\text{out}}$  but less than  $n$  means a trial escape. One can see several trial escapes in Fig. 2. During the escaping time  $\tau_2$ , we can see that  $n_{\text{out}}$  increases from 0 to  $n$  which means a successful escape. The time before the successful escaping event is recorded as the relaxation time  $\tau_1$ .

Most simulations were carried out for a chain of length  $n = 20$  in a system with the *cis* side simulation box is  $20 \times 20 \times 20$  and the *trans* side is  $20 \times 20 \times 50$ . That is  $L_x = L_y = L_z = 20$  is used. Here, the simulation space of the *trans* side in  $z$  direction is always large enough to ensure no boundary effect on the chain. Simulations for a longer chain  $n = 50$  give similar results. In this work, all data of the average translocation time  $\langle \tau \rangle$  as well as average relaxation time  $\langle \tau_1 \rangle$  and the escaping time  $\langle \tau_2 \rangle$  are averaged over at least 500 independent runs. We find that the standard statistical error is less than 3%. In the following figures (except Figs. 4, 5, and 7), the heights of error bars are of the similar sizes of symbols. Therefore we do not include the error bars in these figures.

### 3. Simulation results and discussion

The dependence of average translocation time  $\langle \tau \rangle$  on interaction  $\varepsilon$  is presented in Fig. 3 for different numbers of chain on the *cis* side. An interesting finding is that there exists a minimum translocation time ( $\tau$ ) for an attractive pore. The interaction at which  $\langle \tau \rangle$  is minimum is defined as optimal interaction  $\varepsilon_0$  in this work. While for the interaction above  $\varepsilon$  and below  $\varepsilon_0$ ,  $\langle \tau \rangle$  increases roughly exponentially with the interaction  $\varepsilon$ , indicating that the translocation of chain is very sensitive to the interaction.

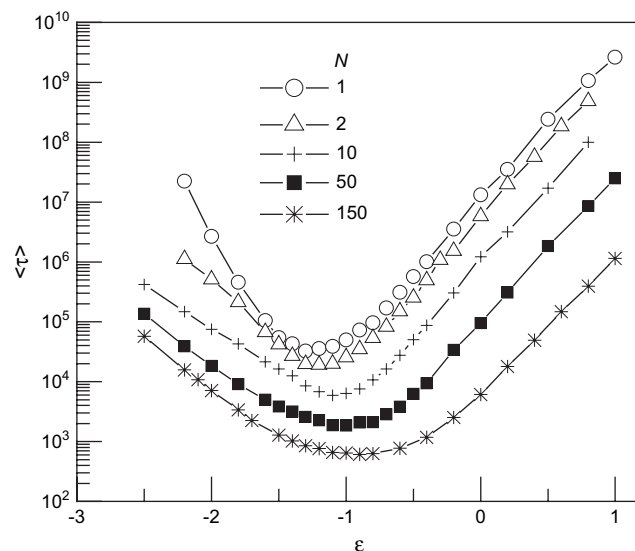


Fig. 3. The dependence of the average translocation time  $\langle \tau \rangle$  of one chain on the interaction  $\varepsilon$  for four situations with numbers of chain  $N = 1, 2, 10, 50$  and 150, respectively. Chain length  $n = 20$ .

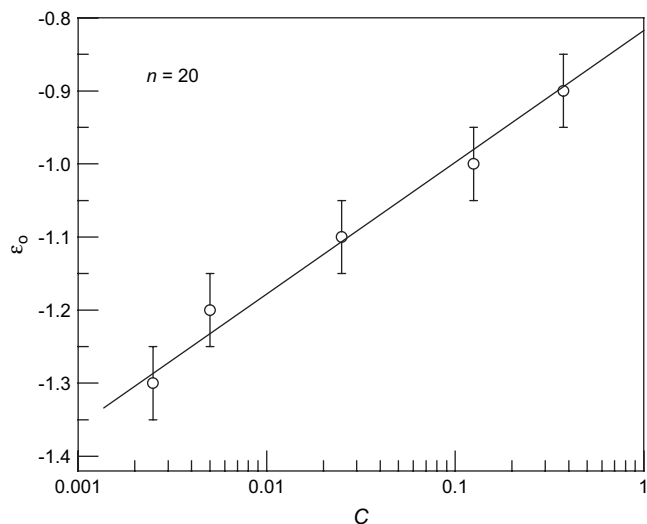


Fig. 4. The dependence of the optimal interaction  $\varepsilon_0$  on the concentration  $C$  of polymer chain. These concentrations correspond to chain numbers  $N = 1, 2, 10, 50$  and  $150$ , respectively, with chain length  $n = 20$ . The straight line is a guide for eyes.

The value of the optimal value  $\varepsilon_0$  depends on the initial chain number  $N$  as well as the chain length  $n$ . For example, for chain length  $n = 20$  the value  $\varepsilon_0$  raises from  $-1.3$  for  $N = 1$  to  $-0.9$  for  $N = 150$ . While for  $N = 1$ , it raises from  $-1.3$  for  $n = 20$  to  $-1.1$  for  $n = 50$ . For chain length  $n = 20$ , the dependence of  $\varepsilon_0$  on concentration  $C$  is presented in Fig. 4. Here the error of  $\varepsilon_0$  is estimated as  $0.05$ , half of the minimum interval of the interaction in our calculations. We find that  $\varepsilon_0$  increases linearly with logarithm of  $C$  within the error, that is,  $\varepsilon_0 \sim \ln C$ .

Probability distributions of translocation time  $\tau$  are counted for non-interacting hole ( $\varepsilon = 0$ ), weak attractive hole ( $0 > \varepsilon > \varepsilon_0$ ), optimal interaction hole ( $\varepsilon = \varepsilon_0$ ) and strong attractive hole ( $\varepsilon < \varepsilon_0$ ), respectively. Fig. 5 gives the probability

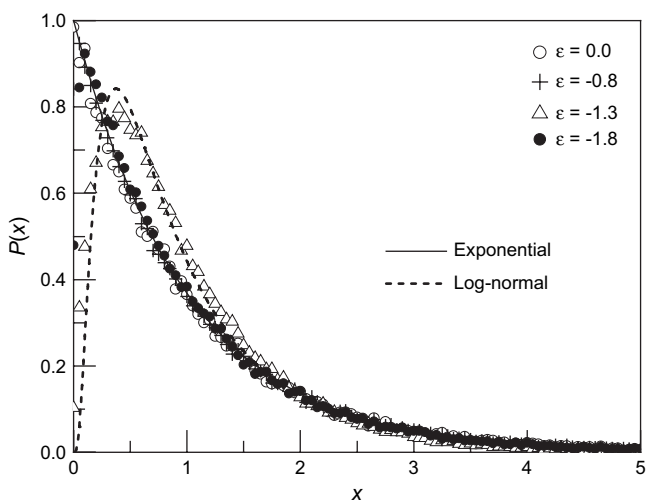


Fig. 5. The probability distribution of scaled translocation time  $P(x)$  with  $x \equiv \tau / \langle \tau \rangle$  for chain length  $n = 20$  at different interactions  $\varepsilon = 0, -0.8, -1.3$  and  $-1.8$ .  $\langle \tau \rangle$  is average translocation time. The solid curve is an exponential decay function and the dashed curve is a Log-normal distribution function.

distributions  $P(x \equiv \tau / \langle \tau \rangle)$  for  $N = 1$  and  $n = 20$  at interactions  $\varepsilon = 0, -0.8, -1.3$  and  $-1.8$ . Here the new variable  $x \equiv \tau / \langle \tau \rangle$  is introduced for convenience. In the calculation, the interval of  $x$  is  $0.05$ . And the distributions  $P(x)$  are normalized to satisfy  $\int_0^\infty P(x) dx = 1$ . For the first two cases ( $\varepsilon = 0$  and  $-0.8$ ), the distributions  $P(x)$  decrease exponentially with  $x$  as

$$P(x) = \exp(-x). \quad (2)$$

While at  $\varepsilon = \varepsilon_0 = -1.3$ , the distribution is found to approach a Log-normal distribution type as

$$P(x) = \frac{1}{\sqrt{2\pi\sigma x}} \exp\left[-\frac{(\ln x - a)^2}{2\sigma^2}\right] \quad (3)$$

with  $a = -0.23$  and  $\sigma = 0.87$ . Here  $a$  and  $\sigma$  are parameters determining the distribution. The distribution takes the maximum at  $x = \exp(a - \sigma^2) = 0.36$ . Probability distributions near  $\varepsilon_0$  can also be roughly described by Log-normal

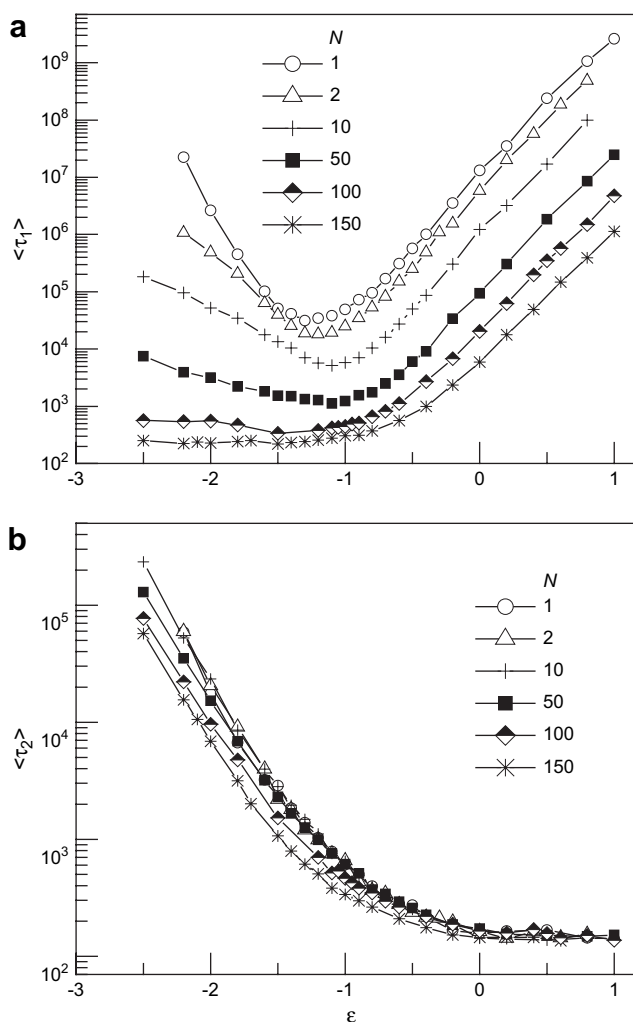


Fig. 6. The dependence of average relaxation time  $\langle \tau_1 \rangle$  (a) and average escaping time  $\langle \tau_2 \rangle$  (b) of one chain on the interaction  $\varepsilon$  for system with different chain numbers  $N = 1, 2, 10, 50, 100$ , and  $150$ . Chain length  $n = 20$ .

distributions with different sets of  $(a, \sigma)$ . For example,  $a = -0.28$  and  $\sigma = 1.1$  can approximately describe the  $P(x)$  curves at  $\varepsilon = -1.1$  and  $-1.7$ . With further increase of the interaction strength to  $\varepsilon = -1.8$ , the distribution roughly becomes  $P(x) = \exp(-x)$  again with a slight deviation near  $x = 0$ . We have also calculated probability distributions for system with  $N = 50$  and  $n = 20$ , and found the same results as that for system with  $N = 1$  and  $n = 20$ . Therefore, we conclude that the distributions of the translocation time  $\tau$  near and away from  $\varepsilon_0$  are different and can be easily distinguished.

The dependences of the average relaxation time  $\langle\tau_1\rangle$  and the average escaping time  $\langle\tau_2\rangle$  on the interaction  $\varepsilon$  are presented in Fig. 6a and b, respectively. When  $N$  is small, the behavior of  $\langle\tau_1\rangle$  is similar to that of the average translocation time  $\langle\tau\rangle$ , i.e.  $\langle\tau_1\rangle$  has a minimum at a moderate attractive interaction near  $\varepsilon_0$ . When  $N$  is large,  $\langle\tau_1\rangle$  is roughly a constant at  $\varepsilon < \varepsilon_0$  and it then increases with  $\varepsilon$  at  $\varepsilon > \varepsilon_0$ . However, the behavior of  $\langle\tau_2\rangle$  is different. It is roughly a constant for

repulsive interaction but it increases gradually with the increase of the attractive strength  $|\varepsilon|$ .

For systems with few chains, e.g.  $N = 1$  or 2,  $\langle\tau_1\rangle$  is much bigger than  $\langle\tau_2\rangle$  for the interaction region we have studied. In this case, chain spends long time on the *cis* side while the final successful escape takes relatively short time. While for system with many chains, e.g.  $N = 50$ , the whole translocation process is dominated by the relaxation process of chain at  $\varepsilon > \varepsilon_0$ , but it is dominated by the final escaping process for strong attractive pore with  $\varepsilon < \varepsilon_0$ .

For a non-interacting pore, it was pointed out that the average escaping time  $\langle\tau_2\rangle$  of a chain through a pore is dominated by chemical potential difference  $\Delta\mu$  between *cis* and *trans* sides [5,8]. Based on nucleation theory, Muthukumar [8] pointed out that the escaping time  $\langle\tau_2\rangle$  could be expressed as

$$\langle\tau_2\rangle \propto \begin{cases} \frac{n^2}{2k_0}, & n\Delta\mu < 1 \\ \frac{1}{k_0\Delta\mu}n, & n\Delta\mu > 1 \end{cases} \quad (4)$$

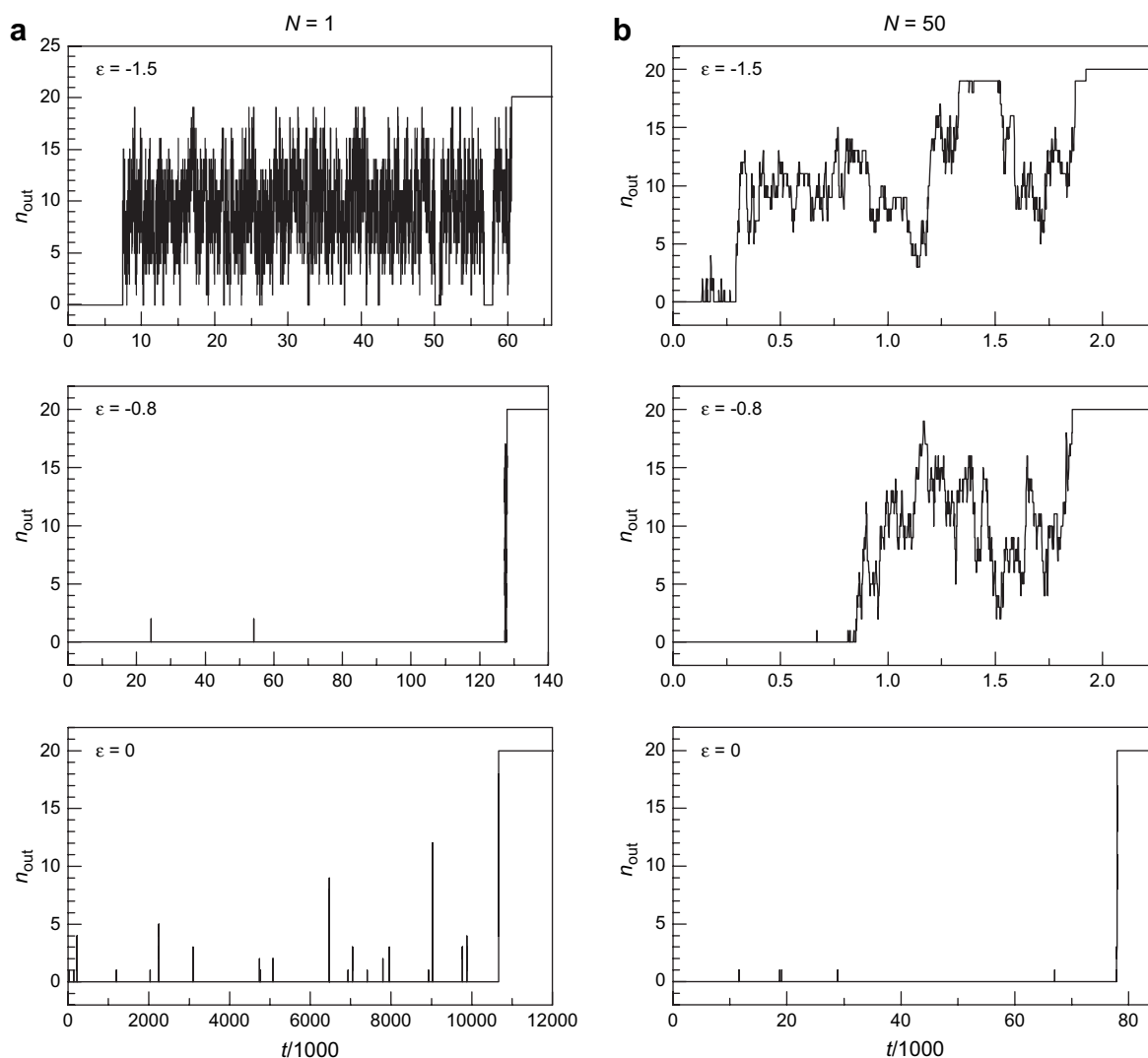


Fig. 7. The variation of segment number out of the box,  $n_{\text{out}}$ , with time  $t$  at different interactions  $\varepsilon$  for two systems with chain numbers: (a)  $N = 1$  and (b)  $N = 50$ . Note different time scales for different interactions and chain lengths. Chain length  $n = 20$ .

where  $k_0$  is a rate constant for transporting a segment across the pore. In our system the chemical potential difference  $\Delta\mu$  is determined by the concentration of polymer on the *cis* side [38], so it is independent of the interaction. Since the escaping time  $\langle\tau_2\rangle$  is dependent on  $\varepsilon$  (Fig. 6b), it therefore means that the rate constant  $k_0$  in Eq. (4) is also dependent on  $\varepsilon$ . We then propose that  $k_0$  decreases with the increase of the attractive strength  $|\varepsilon|$  because  $\langle\tau_2\rangle$  increases with  $|\varepsilon|$  for all attractive holes.

In order to understand the different behaviors of chain at different interactions, we have studied the microscopic behavior of chain during the translocation. We have recorded the variation of the number of segments out of the box,  $n_{\text{out}}$ , for different systems. The typical results for single chain system ( $N=1$ ) and multi-chain system ( $N=50$ ) are presented in Fig. 7 for three interactions:  $\varepsilon = -1.5, -0.8$  and  $0$ .

Qualitatively, both systems show similar behavior. For strong attractive interactions, e.g.  $\varepsilon = -1.5$ , the chain finds the pore easily but spends long time to eventually escape from the pore. We can see that the chain repeatedly goes forward and draws back near the pore because of strong attractive interaction. For a moderate attractive interaction, e.g.  $\varepsilon = -0.8$ , chain easily finds the pore and escapes from the pore after a few trial finding events. For a non-interacting pore  $\varepsilon = 0$  or repulsive pores (not shown), chain spends long time to find the pore and undergoes many trial escaping events before the final escape. Quantitatively, there is a visible difference between these two systems for trial escapes: The value  $n_{\text{out}}$  can be very big for the  $N=1$  system but it is always small for the  $N=50$  system. It is not strange because the system is almost symmetrical for single chain, i.e., it is symmetrical for the chain on both sides. But the symmetry is broken for the multi-chain system. Therefore, value  $n_{\text{out}}$  is always small before the last successful escape for the  $N=50$  system. The inter-chain interaction is clearly revealed.

One can see, from Fig. 7, that one translocation usually contains several trial escapes before the last final escape. Here, the average time elapse for the trial escape is named trial escape time  $t_{\text{esc}}$  and the average time interval between two escapes is named finding time  $t_{\text{find}}$ . During the finding time  $t_{\text{find}}$  one of chains finds the pore and tries to escape. The average relaxation time  $\langle\tau_1\rangle$  is constructed by all finding and trial escaping processes, that is

$$\langle\tau_1\rangle = N_{\text{find}}t_{\text{find}} + (N_{\text{find}} - 1)t_{\text{esc}}. \quad (5)$$

Here  $N_{\text{find}}$  is the total finding events before the final successful escape. The number of trial escapes is  $N_{\text{find}} - 1$  because the last escape is the final successful escape. Each trial escape here corresponds to a blockade of chain in the experiment of DNA transport through a nanopore [6].

Fig. 8a gives the variation of  $t_{\text{find}}$  with interaction  $\varepsilon$  for systems of chain numbers  $N=1$  and  $50$ , respectively. For the single chain system,  $t_{\text{find}}$  increases gradually with  $\varepsilon$ . While for the multi-chain system of  $N=50$ ,  $t_{\text{find}}$  remains roughly constant when  $\varepsilon < \varepsilon_0$ , and then increases with  $\varepsilon$  when  $\varepsilon > \varepsilon_0$ .

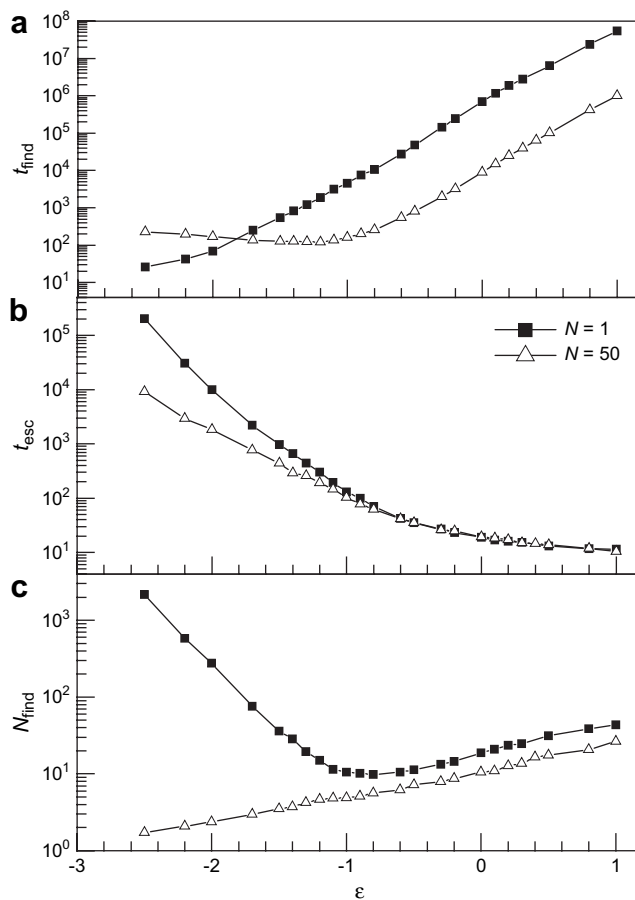


Fig. 8. The dependence of average finding time  $t_{\text{find}}$  (a), average trial escaping time  $t_{\text{esc}}$  (b), and the average number of a chain finding the pore  $N_{\text{find}}$  (c) on the interaction  $\varepsilon$  for two systems with chain numbers:  $N=1$  and  $N=50$ . Chain length  $n=20$ .

Fig. 8b presents the interaction dependence of  $t_{\text{esc}}$ . The average escape time  $t_{\text{esc}}$  decreases with the increase of interaction  $\varepsilon$  for single and multi-chain systems, similar to the curve of the average translocation time  $\langle\tau_2\rangle$  versus the interaction (Fig. 6b). When  $\varepsilon$  is close to zero, the average escape time  $t_{\text{esc}}$  is independent of initial chain number  $N$ , similar to the behavior of  $\langle\tau_2\rangle$  at low concentration (Fig. 6b). A large value of  $t_{\text{esc}}$  for attractive pore means that chain spends long time for transporting, indicating a small transporting rate  $k_0$  in Eq. (4).

Because of the different behaviors of  $t_{\text{find}}$  and  $t_{\text{esc}}$  varying with  $\varepsilon$ , they will intersect at special interaction. We have checked the cross point of curves  $t_{\text{find}} - \varepsilon$  and  $t_{\text{esc}} - \varepsilon$  and found that the cross point is very close to  $\varepsilon_0$ . That is,  $t_{\text{find}} > t_{\text{esc}}$  when  $\varepsilon > \varepsilon_0$  but  $t_{\text{find}} < t_{\text{esc}}$  when  $\varepsilon < \varepsilon_0$ . Therefore, one can see that the average relaxation time  $\langle\tau_1\rangle = N_{\text{find}}t_{\text{find}} + (N_{\text{find}} - 1)t_{\text{esc}}$  is dominated by  $t_{\text{find}}$  for weak attractive and repulsive pores ( $\varepsilon > \varepsilon_0$ ) while it is dominated by  $t_{\text{esc}}$  for strong attractive pores ( $\varepsilon < \varepsilon_0$ ).

Fig. 8c presents the dependence of the average finding events  $N_{\text{find}}$  on the interaction. For the single chain system, the curve is similar to that of the total translocating time  $\tau$ :  $N_{\text{find}}$  at first decreases with the decrease of interaction, then increases when the attraction is strong enough. For multi-chain system,  $N_{\text{find}}$  decreases gradually with the decrease of interaction  $\varepsilon$ .

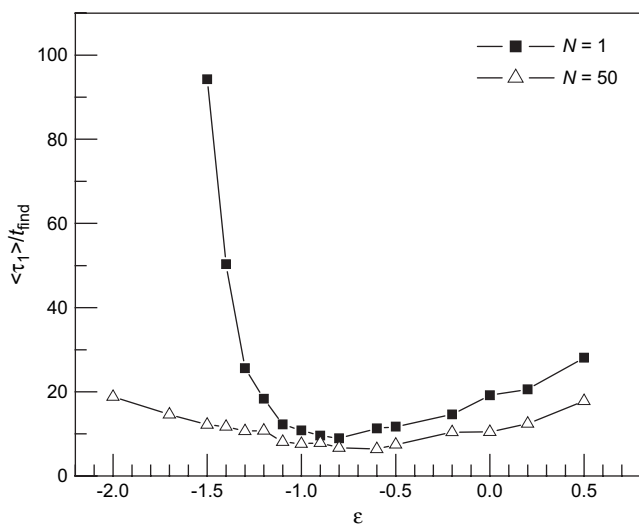


Fig. 9. The dependence of the ratio  $\langle \tau_1 \rangle / t_{\text{find}}$  on the pore–polymer interaction  $\epsilon$  for both single chain system ( $N=1$ ) and multi-chain system ( $N=50$ ). Chain length  $n=20$ .

Based on classical nucleation theory, the average relaxation time  $\langle \tau_1 \rangle$  relates to two main factors: (1) the time interval for chain finds the pore which is  $t_{\text{find}}$  in the simulation, and (2) the energy barrier  $F_b$  of pore [14]. The value  $\langle \tau_1 \rangle$  can then be expressed as

$$\langle \tau_1 \rangle \propto t_{\text{find}} \exp(F_b). \quad (6)$$

The term  $\exp(F_b)$  comes from the assumption that the chain has the probability  $\exp(-F_b)$  to overcome the barrier [14]. Fig. 9 presents the ratio  $\langle \tau_1 \rangle / t_{\text{find}}$  for both single chain system and multi-chain system. We find that the ratio  $\langle \tau_1 \rangle / t_{\text{find}}$  has a minimum at moderate attractive interaction. The results indicate that the value  $\exp(F_b)$  or the barrier  $F_b$  depends on the pore–polymer interaction  $\epsilon$ . However, the reason is not yet clear now. The topic that how does  $F_b$  quantitatively depend on the interaction will be further investigated by calculating the interaction dependence of the free energy landscape.

#### 4. Conclusion

We have investigated the translocation of polymer chains through an interacting nanopore from a high concentration region (*cis* side) to a zero concentration region (*trans* side) by using dynamical Monte Carlo method. The size of chain is much bigger than the size of cross section of pore thus the chain suffers a free energy barrier when it crosses the pore. The driving force for translocation is the concentration difference between the *cis* side and *trans* side. The effect of the pore–polymer interaction  $\epsilon = E/k_B T$  on the translocation of polymer chains is studied. We find that a moderate attractive pore accelerates the translocation of chain. The minimum of average total translocation time  $\langle \tau \rangle$  is located at optimal interaction  $\epsilon_o \sim -1.3$  for single chain system and  $\epsilon_o$  increases linearly with the logarithm of concentration. Our main conclusion is that a proper pore–polymer interaction can drive

chains through nanopores from a high concentration region to a low concentration region. We have also studied the distribution of translocation time  $\tau$ . The distribution of  $\tau$  is a Log–normal distribution function near  $\epsilon_o$  while it is an exponential decay function away from  $\epsilon_o$ .

In this study, the key parameter is scaled interaction  $\epsilon = E/k_B T$ , which relates to the interaction  $E$  and temperature  $T$ . Therefore, our results indicate that one can control the translocation of polymer chain by varying the interaction  $E$  or temperature  $T$ .

According to recent theoretical works, our results also indicate that the transporting rate of chain through nanopore  $k_0$  and the free energy barrier  $F_b$  are dependent on the pore–polymer interaction  $\epsilon$ . However, many questions remain unanswered. Future work will focus on the physical underlying of how the chemical potential difference  $\Delta\mu$  and the free energy barrier  $F_b$  depend on the interaction  $\epsilon$ .

#### Acknowledgement

The project is sponsored by the National Natural Science Foundation of China under Grant No. 20674074.

#### References

- [1] Han J, Turner SW, Craighead HG. Phys Rev Lett 1999;83:1688.
- [2] Henrickson SE, Misakian M, Robertson B, Kasianowicz JJ. Phys Rev Lett 2000;85:3057.
- [3] Meller A, Nivon L, Branton D. Phys Rev Lett 2001;86:3435.
- [4] Kasianowicz JJ, Henrickson SE, Weetall HH, Robertson B. Anal Chem 2001;73:2268.
- [5] Sung W, Park PJ. Phys Rev Lett 1996;77:783.
- [6] Slater GW, Guo HL, Nixon GI. Phys Rev Lett 1997;78:1170.
- [7] Dimarzio EA, Mandell AL. J Chem Phys 1997;107:5510.
- [8] Muthukumar M. J Chem Phys 1999;111:10371.
- [9] Lubensky DK, Nelson DR. Biophys J 1999;77:1824.
- [10] Boehm RE. Macromolecules 1999;32:7645.
- [11] Tian P, Smith GD. J Chem Phys 2003;119:11475.
- [12] Slonkina E, Kolomeisky AB. J Chem Phys 2003;118:7112.
- [13] Chern SS, Cárdenas AE, Coalson RD. J Chem Phys 2001;115:7772.
- [14] Muthukumar M. Phys Rev Lett 2001;86:3188.
- [15] Milchev A, Binder K, Bhattacharya A. J Chem Phys 2004;121:6042.
- [16] Milchev A, Binder K. Comput Phys Commun 2005;169:107.
- [17] Lansac Y, Maiti PK, Glaser MA. Polymer 2004;45:3099.
- [18] Chen C-M. Physica A 2005;350:95.
- [19] Luo MB. Polymer 2005;46:5730.
- [20] Gu F, Wang HJ. Chin Phys Lett 2005;22:2549.
- [21] Ding KJ, Cai DQ, Zhan FR, Wu LJ, Wu YJ, Yu ZL. Chin Phys 2006;15:940.
- [22] Shen Y, Zhang LX. Polymer 2007;48:3593.
- [23] He YD, Qian HJ, Lu ZY, Li ZS. Polymer 2007;48:3601.
- [24] Simon SM, Blobel G. Cell 1991;65:371.
- [25] Akeson M, Branton D, Kasianowicz JJ, Brandin E, Deamer DW. Biophys J 1999;77:3227.
- [26] Helenius J, Ng DTW, Marolda CL, Walter P, Valvano MA, Aebi M. Nature 2002;415:447.
- [27] Alberts B, Bray D. Molecular biology of the cell. New York: Garland; 1994.
- [28] Kasianowicz JJ, Brandin E, Branton D, Deamer D. Proc Natl Acad Sci USA 1996;93:13770.
- [29] Han J, Craighead HG. Science 2000;288:1026.
- [30] Tessier F, Labrie J, Slater GW. Macromolecules 2002;35:4791.
- [31] Chen Z, Escobedo FA. Mol Simul 2003;29:417.

- [32] Panwar AS, Kumar S. *Macromolecules* 2006;39:1279.
- [33] Chang DC. *Guide to electroporation and electrofusion*. New York: Academic; 1992.
- [34] Zimm BH, Levene SD. *Q Rev Biophys* 1992;25:171.
- [35] Yan WW, Kirkland JJ, Bly DD. *Modern size-exclusion liquid chromatography*. New York: John Wiley and Sons; 1979.
- [36] Turner SWP, Cabodi M, Craighead HG. *Phys Rev Lett* 2002;88:128103.
- [37] Huang JH, Mao ZF, Qian CJ. *Polymer* 2006;47:2928.
- [38] Chen YC, Wang C, Luo MB. *J Chem Phys* 2007;127:044904.
- [39] Nakane JJ, Akeson M, Marziali A. *J Phys Condens Matter* 2003;15:R1365.
- [40] Chang H, Venkatesan BM, Iqbal SM, Andreadakis G, Kosari F, Vasmatis G, et al. *Biomed Microdevices* 2006;8:263.
- [41] Gurler MT, Crab CC, Dahlin DM, Kovas J. *Macromolecules* 1983;16:398.
- [42] Wang C, Luo MB. *J Appl Polym Sci* 2007;103:1200.